Available online at www.sciencedirect.com
SCIENCE DIRECT®
Solar Energy Materials & Solar Cells
ELSEVIER
Solar Energy Materials & Solar Cells 78 (2003) 469–491
www.elsevier.com/locate/solmat

Material and solar cell research in microcrystalline silicon

A.V. Shah*, J. Meier, E. Vallat-Sauvain, N. Wyrsch, U. Kroll, C. Droz, U. Graf

Institute of Microtechnology (IMT), University of Neuchâtel, CH-2000 Neuchâtel, Switzerland

Abstract

This contribution describes the introduction of hydrogenated microcrystalline silicon (μc-Si:H) as novel absorber material for thin-film silicon solar cells. Work done at IMT Neuchâtel in connection with deposition of μc-Si:H layers by very high frequency glow discharge deposition is related in detail. Corresponding layer properties w.r.t. material microstructure, hydrogen content, stability and electronic transport are referred to. Basic properties of single-junction, entirely microcrystalline, thin-film silicon solar cells are related: Spectral response, stability w.r.t. light-induced degradation, basic solar cell parameters (V_{oc}, J_{sc} and FF) obtained by IMT Neuchâtel and by other laboratories are listed and commented; the deposition rate issue is addressed. Finally, microcrystalline/amorphous, i.e. "micromorph" silicon tandem solar cells, are described, together with recent developments on the research and industrial front.

Keywords: Microcrystalline silicon; Plasma deposition; Material properties; Electronic transport; Single-junction solar cells; Tandem solar cells

1. Introduction

Hydrogenated microcrystalline silicon (μc-Si:H) was first fabricated in 1968 by Veprek and Maracek [1], it was obtained here by a special kind of plasma-deposition technique, involving chemical vapor transport. Thereafter, Usui et al. [2] as well as Spear et al. [3] reported about μc-Si:H layers obtained by what was later to become the standard form of radio frequency glow discharge employed for the deposition of

*Corresponding author. Tel.: +41-32-718-3335; fax: +41-32-718-3210.
E-mail address: arvind.shah@unine.ch (A.V. Shah).

0927-0248/03/$ - see front matter
doi:10.1016/S0927-0248(02)00448-8

hydrogenated amorphous silicon. Thereby, silane (SiH_4) is used as an original source gas and is strongly diluted with hydrogen, when introduced into the plasma, so as to induce formation of a microcrystalline, rather than of an amorphous lattice structure. In these first experiments, the deposition rates were very low, with values well below 1 Å/s. Such μc-Si:H layers had, in the early days, a strong n-type character; they could also be easily doped, e.g. with phosphine, so as to push the Fermi level upwards towards the conduction band edge and to obtain layers with an even more pronounced n-type character, or with diborane, so as to push the Fermi level downwards towards the valence band edge and to obtain p-type layers. These n- and especially p-type μc-Si:H layers are presently used, both by research laboratories and by production lines, for incorporation within pin-type thin-film silicon solar cells, where the photovoltaically active intrinsic (i) layer consists of hydrogenated amorphous silicon (a-Si:H). They are, in particular, also needed for the tunnel/recombination junctions that form the connection between individual cells, in a double-junction (tandem) or triple-junction a-Si:H solar cell. On the other hand, to use hydrogenated microcrystalline silicon (μc-Si:H) as the photovoltaically active layer within a thin-film solar cell is not straightforward, for two reasons:

- μc-Si:H is a material with an indirect bandgap (like crystalline silicon), and therefore its absorption coefficient in the visible part of the solar spectrum is relatively low, much lower than that of a-Si:H; this means that correspondingly thick μc-Si:H layers are necessary to obtain sufficient absorption and photogeneration;
- electronic transport in microcrystalline silicon layers can be obstructed by the many grain boundaries present in the material—if they are not well passivated by hydrogen.

For these reasons, it took several years before thin-film silicon solar cells with a microcrystalline intrinsic layer (used as photogeneration layer) were attempted. Preliminary work was done by Lucovsky et al. [4], and Faraji et al. [5]. Subsequently, our group successfully pioneered [6–8] entirely microcrystalline pin- and nip-type silicon solar cells fabricated with the very high frequency (VHF) glow discharge method, thereby rapidly attaining AM 1.5 efficiencies higher than 7% [9,10]. Since then, this type of solar cell has been developed further, by our own group and by many other research groups, using different fabrication techniques for the microcrystalline layers. A fully microcrystalline silicon solar cell can be advantageously combined with an amorphous silicon solar cell in a tandem concept called the "micromorph" or "hybrid" concept. Thereby, stable efficiencies between 10% and 12% are reached in the laboratory. Pilot production of corresponding large-area modules has recently been started by a Japanese firm, Kaneka Corp., and large-scale industrial production at the level of several MW/year is now being taken up. Thus, hydrogenated microcrystalline silicon has become an important new photovoltaic material, and is showing its potential right up to the industrial level.

In the present contribution, the authors will first deal with the fabrication and basic properties of intrinsic microcrystalline silicon (μc-Si:H) layers, as used for solar

cells; thereafter, they will elaborate on the development of the μc-Si:H pin-type solar cell and then go over to the microcrystalline/amorphous silicon tandem solar cells, which constitute a major R&D line for achieving future low-cost high-efficiency photovoltaic modules.

2. Plasma deposition and microstructure of hydrogenated microcrystalline silicon (μc-Si:H)

2.1. Deposition of μc-Si:H by very high frequency (VHF) plasma

The large majority of fabrication systems for amorphous and microcrystalline silicon layers are based on capacitively coupled plasma reactors. In these systems, the plasma is (almost always) electrically excited with an AC electrical signal, whose frequency is, in general, equal to the standard value of 13.56 MHz, a value reserved for industrial applications within the RF (radio frequency) range.

By increasing the plasma excitation frequency f_{exc} from 13.56 to around 70 MHz, the deposition rate of device-quality amorphous silicon layers can be increased significantly, by a factor of about 5 (Fig. 1). One thereby also pushes up the "powder limit", i.e. the maximum power level or maximum deposition rate above which a significant amount of powder is formed in the reactor. These effects are linked to a reduction in sheath width and to a change in ion bombardment with increasing plasma excitation frequency f_{exc}: the maximum energy of ions impinging on the growing surface is reduced, as f_{exc} is increased [11,12]; at the same time the ion

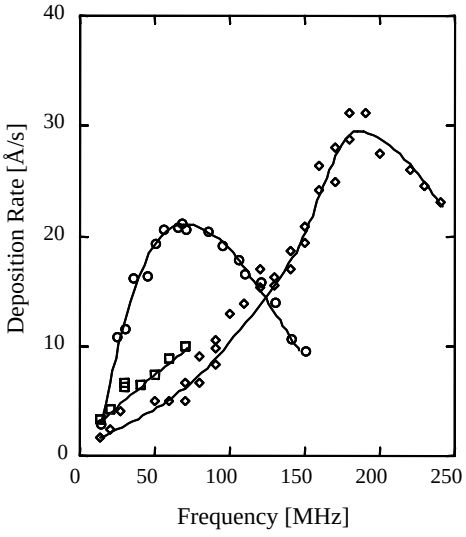

Fig. 1. Deposition rate of amorphous silicon layers vs. plasma excitation frequency, as obtained in different reactors and by independent research groups, according to Ref. [14].

flux is augmented. It now turns out that these phenomena—as prevalent in VHF plasmas—are also propitious to the growth of high-quality μc-Si:H layers at high rates: in Refs. [12,13], the authors have investigated the variation of crystallite size within μc-Si:H layers: the crystallite size increases, as f_{exc} is increased. In a similar manner, as for a-Si:H layers (Fig. 1, [14]), the deposition rate for μc-Si:H layers is also increased for higher values of f_{exc}, although systematic studies on this behavior, over the whole frequency range, have not yet been published.

In our laboratory, the intrinsic layers for our best μc-Si:H solar cells are currently deposited at frequencies around 80–100 MHz and at rates between 4 and 5 Å/s; cells have also been deposited at rates up to 10 Å/s, albeit up to now with a slight reduction in efficiency, e.g. from 7.8% to 6.9% ([8], see also Ref. [15]). Because deposition rate r_d is one of the main existing bottlenecks when one wants to reduce the production cost of μc-Si:H solar cells and modules, the increase of r_d with higher f_{exc} is a significant advantage for an industrial plant. On the other hand, it is difficult to obtain uniform layer deposition over large areas at higher plasma excitation frequencies [16,17]. Thus, large-area (1 m^2 or more) thin-film silicon solar module production by VHF plasma remains a major technical challenge.

2.2. Effect of hydrogen dilution on layer crystallinity and microstructure

In the usual type of glow discharge reactor, the resulting layers are amorphous if deposited from a pure silane plasma. If we add hydrogen to the plasma, we marginally alter the layer quality, whereas the layer remains amorphous until we reach a threshold concentration. If, now, the hydrogen concentration is further increased, we start depositing crystallites, and then the crystalline volume fraction rapidly increases until we obtain layers that are essentially microcrystalline.

By increasing even further the hydrogen dilution of the plasma, we vary the microstructure of the layers; at high values of hydrogen dilution, high columns separated by cracks appear. The general trend, as observed on transmission electron microscope (TEM) micrographs, for layers deposited by VHF plasma on glass substrates, is shown schematically in Fig. 2 [18].

So far, the best microcrystalline solar cells are deposited near the threshold concentration; for very high values of hydrogen dilution, the material does not appear to be usable for solar cells, because of the cracks that can induce shunts in the cells and that appear also to act as channels by which contamination (e.g. oxygen) can enter into the layer.

The evolution of layer crystallinity with increasing hydrogen dilution can also be demonstrated with X-ray diffraction. Results on this same series of layers deposited on glass are given in Fig. 3 [19]; they highlight the sharpness of the transition.

2.3. Seeding zone and substrate dependence of microcrystalline layer growth

Microcrystalline silicon layers show a pronounced non-uniformity in growth direction that can be clearly seen in the TEM micrograph of Fig. 4 [20].

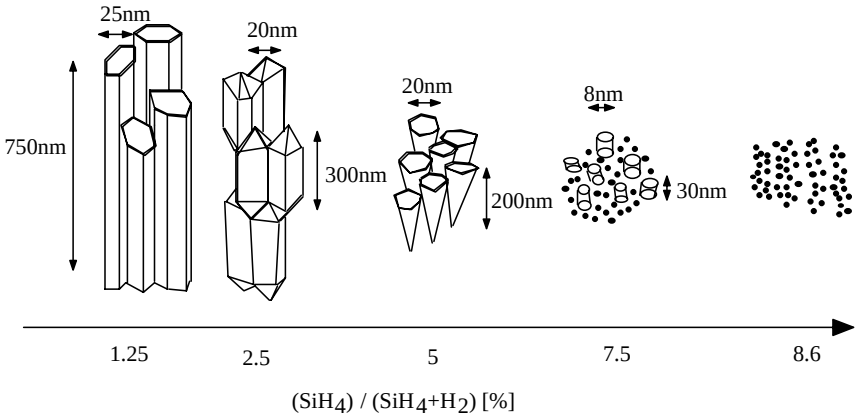

Fig. 2. Schematic evolution of microstructure in microcrystalline silicon (μc-Si:H) with a variation in hydrogen dilution, for layers deposited on glass by VHF-GD. Percentage values refer to concentration of silane in total gas flow (hydrogen + silane); these values decrease for increasing hydrogen dilution [18].

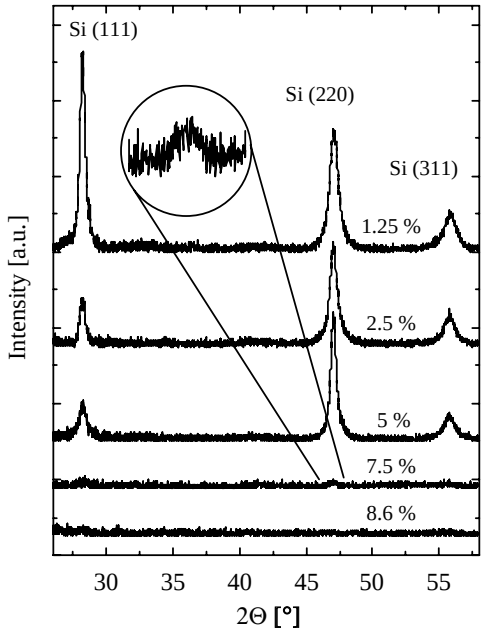

Fig. 3. X-ray diffraction data for a dilution series of μc-Si:H samples deposited on glass substrates; percentage values indicate concentration of silane in total gas flow (hydrogen + silane) [19].

One distinguishes in Fig. 4 (from bottom up) first an amorphous zone, followed by a seeding zone that leads into a hetero-phase region (mixed amorphous/microcrystalline zone) and only thereafter does actual, fully microcrystalline growth starts. The

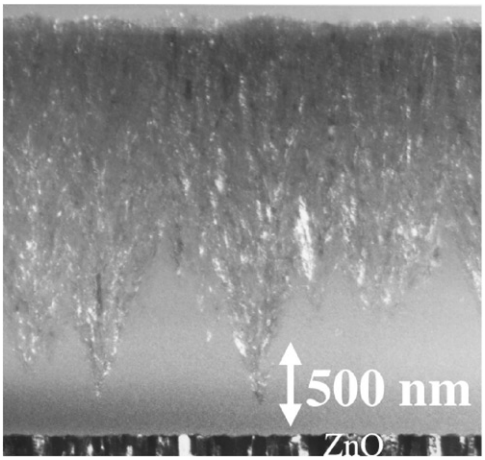

Fig. 4. TEM micrograph of a typical μc-Si:H layer deposited on flat sputtered ZnO [20].

latter zone consists of relatively small crystallites (diameter 20 nm, height more than 100 nm) assembled to form much larger conglomerates.

Because of the importance that nucleation phenomena have for the initial stages of layer growth, it is not surprising that the resulting μc-Si:H layers are sensitively dependent on the substrate and on the underlying layers on which they are grown. Layers that are grown on microcrystalline underlayers tend to be much more crystalline than layers grown on glass. But the situation is even more complex, because the whole growth process depends not only on the crystallinity, but also on the chemical nature and on the crystalline orientation of the underlying layers.

2.4. Some alternative deposition techniques for microcrystalline silicon

A large number of modified, alternative deposition regimes/methods have been studied, primarily with a view to increase the deposition rate of μc-Si:H. Only for a few of these methods have actual solar cell results been confirmed. We would like to mention here just the following two methods:

- Use of higher pressures (up to 10 Torr) and silane depletion conditions (in the so-called HPD, i.e. high-pressure depletion regime) both in connection with RF-plasmas [15] and with VHF-plasmas [21]. Here, the deposition rate can be significantly increased to over 10 Å/s, while still producing high-quality μc-Si:H cells (AM 1.5 efficiencies between 7% and 9% have been reported). Problems prevailing in this regime are: powder formation (see Ref. [15]); high gas consumption, especially of hydrogen (cf. Ref. [22]) and the exceedingly high plasma excitation powers needed, especially in the case of large areas.
- Use of hot wire deposition. Here, high deposition rates (well over 10 Å/s) have indeed been obtained for individual layers [23] and, on the other hand, excellent solar cells (9% efficiency) have been produced, but the latter only at very low

deposition rates [24]. One of the main problems with hot wire deposition for microcrystalline silicon is that the substrate and the growing layer receive thermal radiation from the heated filament and, therefore, deposition temperature control for solar cell fabrication becomes a difficult task. This is especially critical if the substrate is placed near the filament, in order to increase the deposition rate.

3. Material properties of intrinsic microcrystalline silicon (μc-Si:H) layers

3.1. Absorption coefficient vs. photon energy

A typical curve for the as-measured (effective) absorption coefficient of intrinsic μc-Si:H layers is given in Fig. 5 [25] as a function of the photon energy E_{ph}, together with the corresponding curves for intrinsic amorphous silicon (a-Si:H) layers and for monocrystalline silicon wafers (c-Si).

One may note the following points:

- the absorption curve for μc-Si:H closely follows that for c-Si, with a shift towards higher values of the absorption coefficient; this shift is mainly due to light scattering by the rough surface of the μc-Si:H layer [26], it may also partly be due to additional absorption from the amorphous volume fraction contained within the μc-Si:H layers, especially for the spectral region where $E_{ph} > 1.8$ eV;

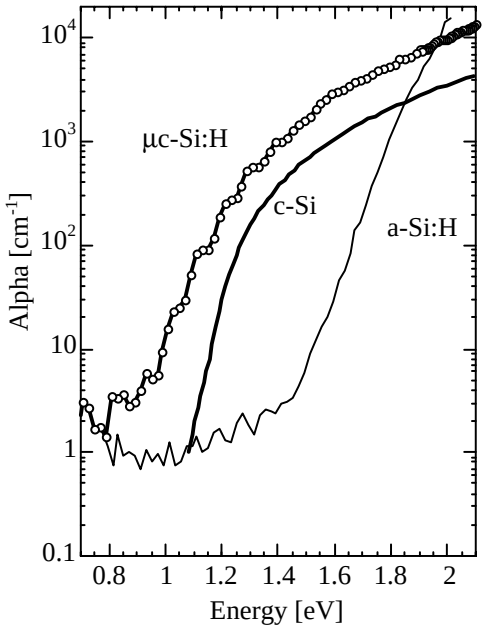

Fig. 5. "Effective" (or "apparent") optical absorption of a μc-Si:H layer deposited by VHF-GD as directly measured by CPM [25] in comparison with amorphous and crystalline silicon.

- the bandgap of μc-Si:H seems to be lower than that of c-Si material, but this effect can be shown to be entirely due to the light scattering effects mentioned above; if a correction for light scattering is carried out, the same bandgap E_g of 1.12 eV can be confirmed for both μc-Si:H layers as for c-Si wafers;
- subbandgap absorption (for $E_{ph} \approx 0.6$ to 0.8 e.V.) of device-quality μc-Si:H layers, as deposited, e.g. by VHF-GD is very low; as-measured values are in the range 1–10 cm^{-1}, because light-scattering on the rough μc-Si:H layer surface increases the as-measured absorption coefficient, the "true" absorption coefficient is often about a factor 10 lower, as can be shown both by optical modeling and by mechanical polishing of the rough surface [26]. Such low values of subbandap absorption are an indication that defect densities in these layers are relatively low, probably quite a bit lower than that for the best obtainable a-Si:H layers; they are certainly an indication that grain boundaries are well passivated by hydrogen in these layers.

For the application of μc-Si:H layers within solar cells, the increase in "effective" or "apparent" optical absorption due to light scattering by the rough surface is beneficial, because it basically allows the solar cell thickness to be reduced. The exact amount of light scattering/light trapping within a full solar cell structure will, however, be rather different from what is measured for an individual layer directly adjacent to air.

3.2. Light-induced degradation and post-oxydation effects

3.2.1. Light-induced degradation

The Staebler–Wronski effect or light-induced degradation effect is prevalent among all types of amorphous silicon (a-Si:H) layers and solar cells produced so far. It came therefore as a surprise that microcrystalline silicon (μc-Si:H) solar cells generally do not show any light-induced degradation. The corresponding μc-Si:H intrinsic layers are certainly also stable w.r.t. the Staebler–Wronski effect (see Refs. [27,28]). A word of caution is, however, called for: the term "μc-Si:H" covers a large variety of different materials, having notable differences in microstructure, crystallite orientation and form and crystalline/amorphous volume fraction. It should not be ruled out that certain types of microcrystalline silicon layers may suffer from light-induced degradation. Indications for this can be found in Ref. [29,30].

3.2.2. Post-oxidation

On the other hand, μc-Si:H layers do suffer from another potential source of instability, i.e. from an increasing contamination by oxygen, when exposed to air over a period of weeks or longer. This so-called "post-oxidation" effect induces a change in the Fermi level E_f which is thereby pushed towards the conduction band edge; because of this, long-term electrical transport and even electrical conductivity measurements on μc-Si:H layers are delicate. One may, if one simply waits for several weeks, detect variations, e.g. in photoconductivity σ_{photo} or dark conductivity

σ_{dark}, which are due to post-oxydation and completely mask whatever other effect one wishes to observe. Fig. 6 [31] shows, as an illustrative example, a particularly pronounced case of post-oxydation on a μc-Si:H layer deposited at high plasma power by VHF-GD.

We suspect that μc-Si:H layers produced with high plasma power and strong hydrogen dilution should generally be more susceptible to post-oxydation, because of the cracks present in them, than the more compact μc-Si:H layers produced near the a-Si:H–μc-Si:H transition [32]. Even though post-oxydation is a severe problem for μc-Si:H layer measurements, μc-Si:H solar cells have shown to be unaffected by this problem. This may partly be due to the type of μc-Si:H material used for entire solar cells, but also, and mainly, due to the sealing effects provided by the relatively thick TCO (transparent conductive oxide) and metallic contact layers, on both sides of the cell.

3.3. Hydrogen in μc-Si:H layers

Hydrogen plays an essential role for defect passivation (dangling bond passivation in a-Si:H and grain boundary passivation in μc-Si:H). Hydrogen is also involved in the process of light-induced degradation in a-Si:H. It is therefore of interest to investigate hydrogen incorporation in different μc-Si:H layers and compare the data with that from corresponding a-Si:H layers.

Hydrogen content for a whole series of a-Si:H and μc-Si:H layers deposited at different values of hydrogen dilution, is reported in Ref. [33]; the hydrogen content is

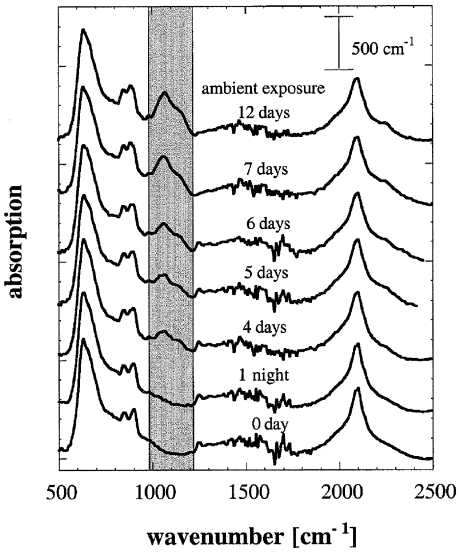

Fig. 6. Successive infrared absorption spectra of a μc-Si:H layer during exposure to air for a period up to 12 days: Increasing oxygen contamination, i.e. post-oxydation, can be clearly seen by the increase in absorption in the range 1000–1200 cm^{-1} (from [31]).

thereby evaluated by IR (infrared) spectroscopy (yielding the content of bonded hydrogen) and by ERDA (elastic recoil detection analysis; yielding the total amount of bonded and non-bonded hydrogen).

The main results are shown in Fig. 7; it is evident that there is much less hydrogen (both bonded and non-bonded) in μc-Si:H layers than in corresponding a-Si:H layers. Kroll et al. [33] also conclude, from a detailed analysis of the peak position in the IR spectra, that for μc-Si:H layers the hydrogen is preferentially bonded at the surface of the microcrystalline grains, and to a lesser extent in the amorphous fraction of the volume. These findings may possibly constitute the first part of a clue needed to explain the difference in light-induced degradation behavior, between a-Si:H and μc-Si:H.

3.4. Electrical transport in μc-Si:H layers

3.4.1. Coplanar transport (steady state)

Mobility lifetime products ($\mu\tau$ products) can be conveniently determined, for the case of a-Si:H layers, from the values of photoconductivity σ_{photo} and ambipolar diffusion length L_{amb}, as measured in a coplanar configuration on the layer surface [34]. The same experimental techniques, namely SSPC (steady-state photoconductivity) and SSPG (steady-state photoconductive grating) can also be applied to μc-Si:H layers.

The results found for a large number of different μc-Si:H layers are shown in Fig. 8 [31,35], as a function of the parameter b, as defined, e.g. in Ref. [36]. Note that

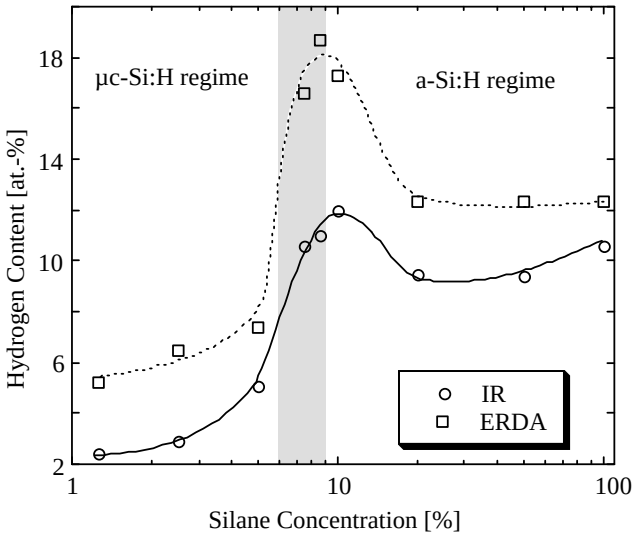

Fig. 7. Hydrogen content for a whole series of μc-Si:H layers deposited at various values of hydrogen dilution, i.e. at various values of silane concentration as determined by IR spectroscopy (bonded hydrogen) and ERDA (bonded and non-bonded hydrogen). Data taken from Ref. [33].

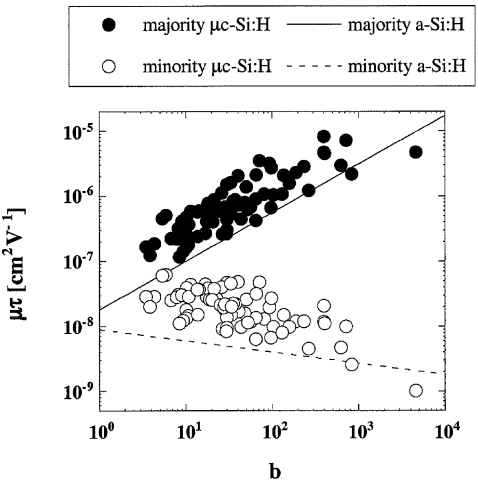

Fig. 8. μτ products for majority carriers (deduced from σ_{photo} measurements) and for minority carriers (deduced from L_{amb} measurements) plotted as a function of the parameter b (indicative of Fermi-level position) for a large number of μc-Si:H samples. Lines show typical values for device-quality, undegraded a-Si:H layers; from Ref. [31].

the parameter b is deduced from σ_{photo} and L_{amb} and constitutes an indication of the Fermi level position in the sample that is being investigated. There is a striking similarity between the results for a-Si:H and μc-Si:H layers. This similarity has been confirmed by further, more detailed investigations [37]. All these observations lead us to the conclusion that electrical transport (at least in coplanar direction and on the top of 1 μm to 2 μm thick layers) is governed by the same factors in both a-Si:H and μc-Si:H—by amphoteric dangling bonds acting as recombination centers, probably located for μc-Si:H layers at the grain boundaries and in the amorphous tissue between grains/conglomerates (see also Ref. [38]). One also concludes that $\mu\tau$ products for coplanar transport in device-quality μc-Si:H layers are equivalent to those of undegraded a-Si:H layers.

3.4.2. Transport in growth direction (steady state)

The diffusion length L_{diff} of minority carriers in growth direction can be measured for μc-Si:H layers by the SPV (surface photovoltage) technique. Values in the range of 0.1–1 μm have been found [39–41].

A comparison between L_{amb} measured by SSPG in coplanar direction (see above) and L_{diff} measured by SPV in growth direction, on the same μc-Si:H samples, is shown in Fig. 9 [41]. It indicates that transport anisotropy in μc-Si:H is not a general phenomenon, but is restricted to particular cases only.

3.4.3. Drift mobilities (transient transport)

Carrier drift mobilities as measured by time of flight constitute important parameters in evaluating thin-film semiconductors w.r.t. transient transport, i.e. to a

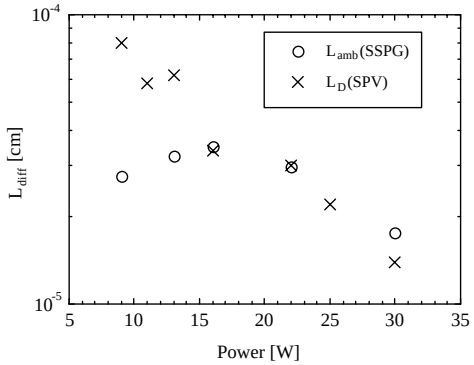

Fig. 9. Comparison between minority carrier/ambipolar diffusion lengths in growth direction (SPV technique) and in coplanar direction (SSPG method) for a few μc-Si:H samples [41].

transport mode where not only the mobile carriers but also the trapped charge plays an essential role.

Results obtained for μc-Si:H and a-Si:H samples fabricated with different dilution levels are given in Ref. [27]. The values obtained there for hole drift mobilities on μc-Si:H samples are about two orders of magnitude higher than those obtained for a-Si:H samples. This would indicate that trapped charge in the valence bandtail is very much lower for μc-Si:H than for a-Si:H (at least for state of the art, device-quality layers). This constitutes an essential advantage that enables one to fabricate p-channel μc-Si:H thin-film transistors [42]. It may also contribute in maintaining a relatively uniform internal field in the i-layer of pin/nip solar cells.

4. Single-junction microcrystalline silicon solar cells

4.1. General structure and spectral response

As seen in Section 3.4 of this paper, the minority carrier/ambipolar diffusion lengths in hydrogenated microcrystalline silicon (μc-Si:H), are, even for the best intrinsic layers, lower than 1 μm. Diffusion lengths in doped layers have so far not been measured, but will probably be even quite a bit lower than those in intrinsic layers.

This means that it is not feasible to form a μc-Si:H solar cell with a pn-diode, because in such a diode the collection of photogenerated carriers is maintained by diffusion. We will instead have to use pin- (or nip-)-type diodes, similar to those used for a-Si:H solar cells, in order to obtain drift-assisted collection, at least in short-circuit conditions. Fig. 10 shows a schematic cross-section of a corresponding pin-diode deposited on a glass substrate and Fig 11a) the spectral response of a μc-Si:H pin-type solar cell, compared with that of an a-Si:H pin-type solar cell. The enhanced response in the near-infrared region (700–1000 nm) is clearly visible. If oxygen is incorporated into the i-layer during deposition, the oxygen-atoms can act as donors,

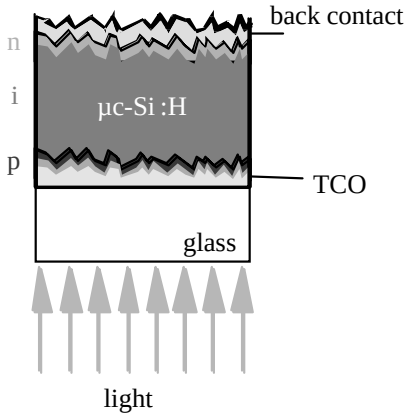

Fig. 10. Typical p-i-n structure for μc-Si:H solar cells.

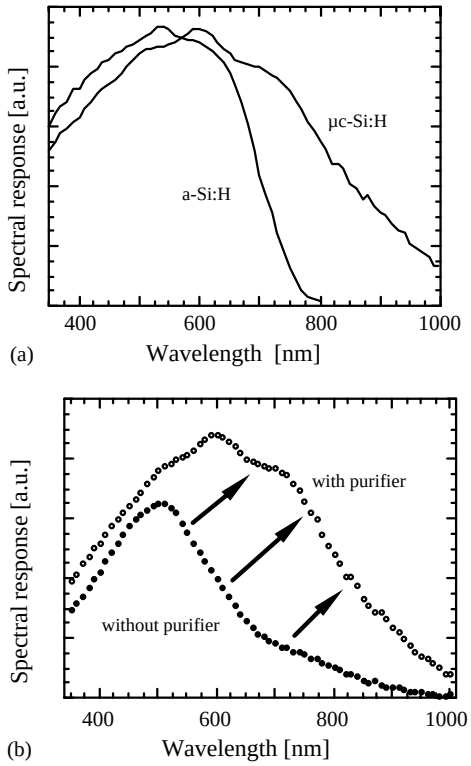

Fig. 11. Spectral response curves of pin-type solar cells: (a) comparison between a typical amorphous silicon and a typical microcrystalline silicon solar cell. (b) Comparison between two μc-Si:H solar cells (i-layer thickness 2.8 μm)—one fabricated without a gas purifier and having an oxygen content of about 10^{20} atoms/cm^3 and the other with a gas purifier and a reduced oxygen content of less than 10^{19} atoms/cm^3 [43].

they are positively ionized during normal solar cell operation and this positive charge can lead to a breakdown of the internal electrical field and of drift-assisted collection within the i-layer; thereby the red and near-infrared response is significantly reduced as illustrated in Fig. 11b) [43]. The detrimental effect of oxygen on collection in the intrinsic (i)-layer of a μc-Si:H pin-type solar cell certainly depends on the way oxygen is incorporated into the silicon crystallites. In a recent publication by the Tsukuba group [44], the authors report on manufacturing μc-Si:H solar cells at lower temperatures and claim excellent performance ($\eta = 8.9\%$) for cells deposited with relatively high oxygen content in the i-layer (2×10^{19} atoms/cm^3, as measured by SIMS). The authors propose that the oxygen atoms are largely "passivated" by hydrogen, and, thus, do not act as donors. This proposition is yet to be substantiated by comparing spectral response curves. The authors attribute the passivation effect (so far not seen elsewhere), to the relatively low deposition temperatures used by them (around 140° instead of 200°C or more, as for most other work). It remains to be seen whether this is feasible in the industrial context, where entire modules with tandem cells have to be fabricated and other process steps may impose higher temperatures.

4.2. Stability

4.2.1. Stability w.r.t light exposure

It was already stated that no Staebler–Wronski effect has been detected in device-quality μc-Si:H layers so far. Fig. 12 [9] shows the comparative behavior—under strong light exposure, of a μc-Si:H solar cell and an a-Si:H solar cell, both with relatively thick i-layers.

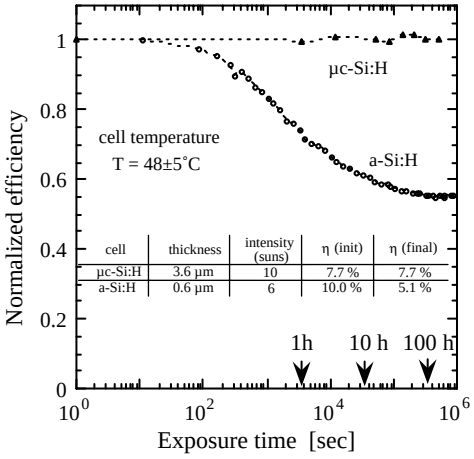

Fig. 12. Comparative behavior of a microcrystalline silicon (μc-Si:H) solar cell and an amorphous silicon (a-Si:H) solar cell under intensive light illumination, from a sodium lamp. Efficiencies were measured before/after light soaking under standard conditions [9].

4.2.2. Stability w.r.t chemical contamination

Individual μc-Si:H layers suffer from post-oxydation, as indicated in Section 3 above. However, it has been shown [45] that in a full pin-type μc-Si:H solar cell, the back contact (consisting of transparent conductive oxide/metal contact layers) acts as a diffusion barrier and prevents post-oxydation: In an experiment, where an individual i-layer and a p-i-n cell incorporating a similar i-layer were both subjected to 70 days of air exposure, the following results were obtained: the individual layer showed a drastic increase in its dark conductivity value σ_{dark}, from 10^{-7} upto $10^{-4}(\Omega\,cm)^{-1}$ and a substantial decrease in the activation energy of σ dark from 520 to 170 meV, both these observations indicating a strong contamination due to a n-type dopant (in this case certainly oxygen). In contrast, the pin cell demonstrated a remarkably constant efficiency value (Fig. 13).

4.3. Cell performance

In order to optimize μc-Si:H single-junction cell performance, we have to act on all three key parameters of the solar cell: on V_{oc}, FF and J_{sc}.

4.3.1. Open-circuit voltage V_{oc}

It has been shown that the open-circuit voltage V_{oc} of typical μc-Si:H solar cells, is governed mainly by interface effects and less by bulk recombination: this was

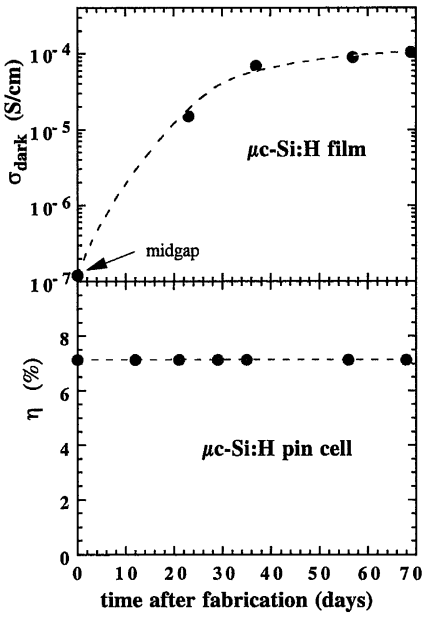

Fig. 13. Comparison of an intrinsic μc-Si:H film and the corresponding p–i–n solar cell in function of air exposure after deposition. The film was characterized by the dark conductivity measurement and the cell by $I-V$ measurements under AM 1.5. The dashed lines are drawn to guide the eye [45].

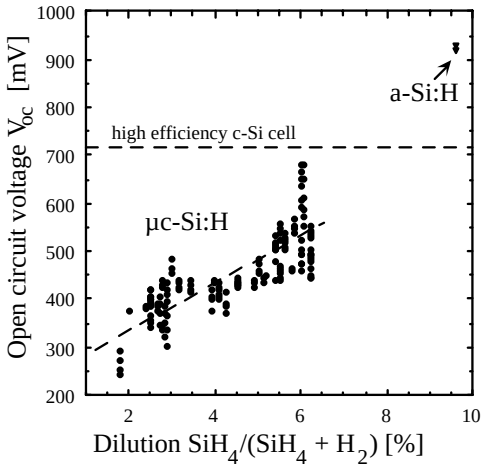

Fig. 14. Open-circuit voltage V_{oc} for a large number of single-junction μc-Si:H pin solar cells deposited at IMT Neuchâtel, from Ref. [46].

demonstrated by Ref. [45], where an experiment was carried out involving two different pin cells co-deposited with identical parameters except for the i-layer thickness, the latter being varied between 0.8 and 3.2 μm by use of a shutter during i-layer deposition: both cells had strictly the same value of V_{oc}.

On the other hand, μc-Si:H cells that are deposited with plasma parameters that are near to those prevalent for the a-Si:H/μc-Si:H transition clearly have higher V_{oc} values, as shown in Fig. 14 [46].

4.3.2. *Fill factor (FF)*

Values of FF reported for state of the art μc-Si:H solar cells range between 70% and a record value of 77%, obtained with a nip cell deposited by plasma at higher temperatures [47]. Three different factors limit the value of FF: (a) insufficient collection within the i-layers; (b) series resistance in the contact layers and (c) shunt paths, both within the bulk of the μc-Si:H solar cell and also on its edge, where grooves are usually cut by laser-scribing. Such shunts are relatively common in μc-Si:H solar cells and constitute a topic for further in-depth research. They can be detected by measuring the solar cell at low light intensities: if FF and V_{oc} show a drastic drop as the light intensity is decreased, this is an indication of an electrical shunt. Because certain types of μc-Si:H layers exhibit cracks, shunts can constitute here a more pronounced problem than in other thin-film solar cells.

4.3.3. *Short-circuit current* (J_{sc})

J_{sc} of a μc-Si:H cell depends mainly on two factors: (a) the thickness d_i of the intrinsic layer and (b) the "light trapping" effect obtained within the entire solar cell through surface roughness of both the microcrystalline silicon layers and of

the contact layers (TCO, metal contacts, substrate surface). In practice, J_{sc} values between 22 and 30 mA/cm^2 have been reported [47–49] for $d_i = 1$–3 μm. Because of the relatively high conductivity of μc-Si:H, special care has to be taken, when determining J_{sc}, to avoid wrongly including, in the measured value of J_{sc}, photogenerated current laterally collected from adjoining areas of the solar cells, areas that do not lie directly under the electrode layer [50]. To avoid such measurement errors, μc-Si:H solar cells for which J_{sc} values are reported should have a large enough area (1 cm^2 or more), and be electrically isolated (by laser scribing or another method of cell structuring) from the adjoining parts of the μc-Si:H layer. Such precautions have not always been taken.

The short-circuit current J_{sc} bears the largest potential for further enhancement and for boosting the cell's overall efficiency: With full absorption of all photons having energies above the bandgap E_g, values for J_{sc} over 40 mA/cm^2 would basically be possible. It is, however, not at all clear whether corresponding high-performance light trapping schemes can indeed be implemented in order to enhance absorption in thin μc-Si:H cells and attain J_{sc} values of more than 30 mA/cm^2. Their investigation constitutes therefore a major research task for the near future.

4.4. *Efficiency values obtained*

At the present time, a large number of laboratories have reported efficiency values in the range 8.5–10.9% for AM 1.5 illumination and measurement temperatures around 25°C (see e.g. Refs. [24,47–49]).

An interesting question is the behavior of μc-Si:H cells at higher temperatures. It appears that μc-Si:H solar cells with high V_{oc} values show a less pronounced drop in efficiency as the temperature increases, than wafer-based crystalline silicon (c-Si) solar cells (Fig. 15, [48]). This feature is of special interest for the practical application of future μc-Si:H-based solar modules.

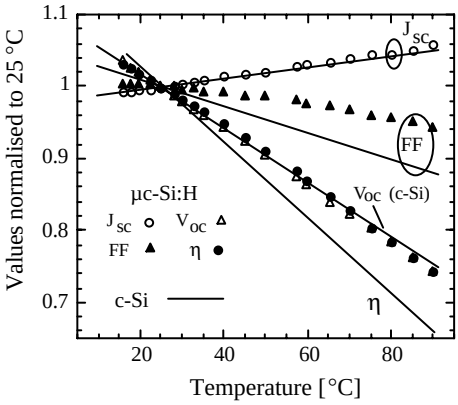

Fig. 15. Temperature behavior of a high-V_{oc} μc-Si:H cell compared with that of a c-Si cell, according to Ref. [48].

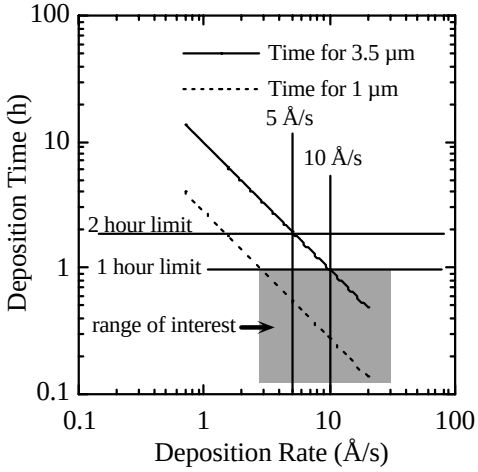

Fig. 16. Deposition time for μc-Si:H films as a function of the deposition rate. The dashed region represents the field of interest for solar cell production [51].

4.5. The deposition time issue

Already for a-Si:H solar module production, silicon deposition time within the plasma reactor constitutes a major factor that influences production costs. μc-Si:H solar cells being substantially thicker than a-Si:H solar cells, deposition times are even more critical in the microcrystalline case. Truly desirable values of around 10–15 min deposition time can only be obtained if both the cell thickness is reduced (to around 1 μm, through suitable light trapping schemes) and the deposition rates are increased (to over 10 Å/s) by novel deposition techniques [51]: This is schematically shown in Fig. 16.

5. Microcrystalline/amorphous ("micromorph") tandem solar cells

5.1. General principle

Tandem and triple-junction solar cells are extensively used in amorphous silicon technology to obtain higher stabilized efficiencies than those attainable with single-junction solar cells. Tandem solar cells are especially attractive, if the bandgap of each component cell can be properly adjusted. For amorphous silicon/amorphous silicon–germanium tandems, a major problem is that it has so far not been possible to include a satisfactory, stable component cell with a bandgap much lower than 1.5 eV. With the introduction of microcrystalline silicon, we now have a fully stable photovoltaic thin-film material with a bandgap of 1.12 eV that can be fabricated in the same manner as amorphous silicon and its bandgap of approximately 1.7–1.8 eV. These values are very near the optimum bandgap combination for tandem cells,

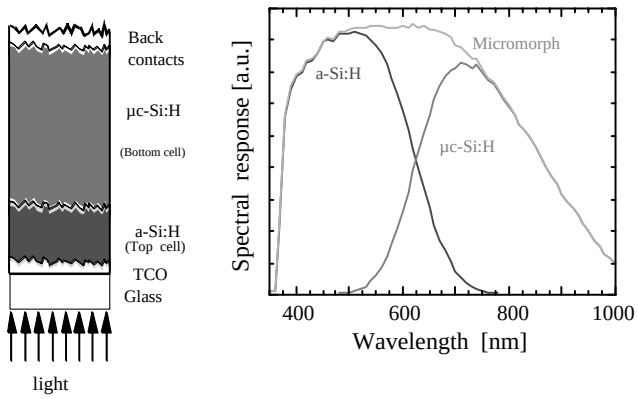

Fig. 17. Schematic structure and corresponding typical spectral response of a microcrystalline/amorphous ("micromorph") tandem silicon solar cell.

as reported, e.g. in Refs. [52,53]. The microcrystalline/amorphous tandem or "micromorph" tandem cell is therefore a particularly interesting combination for thin-film silicon solar cell technology.

The resulting cell structure is shown in Fig. 17, along with the typical spectral response curve of such a tandem.

IMT Neuchâtel introduced this novel tandem solar cell concept and reported first results in 1994 [54]. In 1997, stabilized efficiencies higher than 10% had already been confirmed and reported [55]. A feature of great interest is that all semiconductor layers for these micromorph tandem cells can be fabricated by plasma deposition and at low deposition temperatures of 200°C.

5.2. Present results

A typical I/V curve of a micromorph tandem cell as fabricated recently by our group is shown in Fig. 18.

Other groups have in the meantime obtained similar results [15,47]. Stabilized AM 1.5 efficiencies around 11% are attainable on the laboratory scale. Complete large-area modules (approximately $\frac{1}{2}\,m^2$ size) from industrial production [56,57] have aperture area efficiencies with initial values clearly higher than 10%. Their stabilized values can be assumed to be over 8%. Given that these tandem cells constitute a relatively recent development, it is noteworthy that they already surpass the average efficiency values presently obtained for industrial production of tandem and triple-junction modules in the "conventional" amorphous silicon/amorphous silicon–germanium technology.

5.3. Present issues for cell design

The following are the main factors affecting at present the performance of micromorph tandem cells.

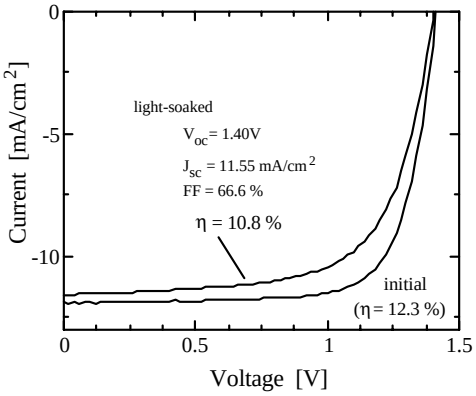

Fig. 18. Typical $I(V)$ curve of micromorph tandem cell from IMT-Neuchâtel (initial and degraded states).

5.3.1. Cell stability

The microcrystalline bottom cell is stable, but the amorphous top cell suffers from the light-induced degradation effect. Therefore, the amorphous top cell must be kept thin enough (about 0.3 μm), so as to avoid excessive efficiency loss during cell stabilization. Because of this, short-circuit currents of the amorphous top cell are rather low and may limit the tandem's performance.

5.3.2. Deposition time

In order to keep the deposition/fabrication time of the microcrystalline bottom cell within reasonable limits, one has to keep its thickness also low (below 1.5 μm). This means that the short-circuit current of the microcrystalline bottom cell is restricted and may, in its turn, limit the tandem's performance.

5.3.3. Current matching and its effects

If the tandem is top-cell limited, it suffers quite substantially from light-induced degradation, but it will have a favorably low temperature coefficient. If, on the other hand, the tandem is bottom-cell limited, then it can be fully stable w.r.t. light-induced degradation [58], but it may be expected to have a higher temperature coefficient.

This means that micromorph tandem cells should be designed for optimal stabilized performance (maximum power rating over the year) under given outdoor conditions (light intensity and spectrum, temperature) and not for standard test conditions. Such a field-oriented cell/module optimization is yet to be undertaken.

5.3.4. Light trapping schemes

To increase the current of micromorph tandems the most promising method is, as of now, to enhance light trapping within the solar cell: An "intermediate mirror layer" between the amorphous top cell and the microcrystalline bottom cell is an interesting scheme that has been tried in this context [56,59,60]. Another, more straightforward scheme is to use enhanced light scattering by the transparent contact

layer, e.g. by an as-grown rough ZnO layer fabricated by low-pressure chemical vapor deposition [58].

6. Conclusion

Hydrogenated Microcrystalline silicon, deposited at low temperatures ($\approx 200^{\circ}C$), from a silane plus hydrogen plasma, is a material that has recently become of prime interest for thin-film solar cells and other thin-film devices. Because of its lower bandgap, it constitutes a useful complement to amorphous silicon. Its basic stability w.r.t. light-induced degradation makes it especially attractive for photovoltaic and optoelectronic applications. However, many fundamental issues relating to the physics of this material are still to be investigated. As for device applications, we may expect further rapid progress in device design and implementation as well as in fabrication technology. It is probably only 4–5 years from now that the full potential of microcrystalline silicon will be realized.

Acknowledgements

The authors gratefully acknowledge financial support of their work from the Swiss "Office federal de l'énergie (OFEN)", and "Fonds national (FN)". They express their thanks to all members of the IMT Neuchâtel thin-film silicon/photovoltaics group, especially to Ms. Sylvie Baillod for manuscript preparation and Mr. Mirko Nagel for manuscript checking.

References

[1] S. Veprek, V. Marecek, Solid State Electron. 11 (1968) 683.
[2] S. Usui, M. Kikuchi, J. Non-Cryst. Solids 34 (1979) 1.
[3] W.E. Spear, G. Willeke, P.G. LeComber, A.G. Fitzgerald, J. Phys-Paris 42 (1981) C4.
[4] G. Lucovsky, C. Wang, R.J. Nemanich, M.J. Williams, Sol. Cells 30 (1991) 419.
[5] M. Faraji, S. Gokhale, S.M. Choudhari, M.G. Takwle, S.V. Ghaisas, Appl. Phys. Lett. 60 (1992) 3289.
[6] R. Flückiger, J. Meier, H. Keppner, U. Kroll, A. Shah, O. Greim, M. Morris, J. Pohl, P. Hapke, R. Carius, Proceedings of the 11th EC PV Solar Energy Conference, Montreux, 1992, p. 617.
[7] J. Meier, R. Flückiger, H. Keppner, A. Shah, Appl. Phys. Lett. 65 (1994) 860.
[8] L. Feitknecht, O. Kluth, Y. Ziegler, X. Niquille, P. Torres, J. Meier, N. Wyrsch, A. Shah, Sol. Energy Mater. Sol. Cells. 66 (2001) 397.
[9] J. Meier, P. Torres, R. Platz, S. Dubail, U. Kroll, J.A.A. Selvan, N. Pellaton-Vaucher, C. Hof, D. Fischer, H. Keppner, A. Shah, K.-D. Ufert, P. Giannoulès, J. Köhler, Proc. Mater. Res. Soc. Symp. 420 (1996) 3.
[10] P. Torres, J. Meier, M. Goetz, N. Beck, U. Kroll, H. Keppner, A. Shah, Proc. Mater. Res. Soc. Symp. 452 (1997) 883.
[11] A.A. Howling, J.L. Dorier, C. Hollenstein, U. Kroll, F. Finger, J. Vac. Sci. Technol. A 10 (1992) 1080.

[12] R. Flückiger, J. Meier, G. Crovini, F. Demichelis, F. Giorgis, C.F. Pirri, E. Tresso, J. Pohl, V. Rigato, S. Zandolin, F. Caccavale, Proc. Mater. Res. Soc. Symp. 358 (1995) 751.
[13] F. Finger, P. Hapke, M. Luysberg, R. Carius, H. Wagner, Appl. Phys. Lett. 65 (1994) 2588.
[14] U. Kroll, A. Shah, H. Keppner, J. Meier, P. Torres, D. Fischer, Sol. Energy Mater. Sol. Cells 48 (1997) 343.
[15] B. Rech, T. Roschek, T. Repmann, J. Müller, R. Schmitz, W. Appenzeller, Thin Solid Films, 2003, in press.
[16] U. Kroll, D. Fischer, J. Meier, L. Sansonnens, A. Howling, A. Shah, Proc. Mater. Res. Soc. Symp. 557 (1999) 121.
[17] L. Sansonnens, A.A. Howling, C. Hollenstein, Proc. Mater. Res. Soc. Symp. 507 (1998) 541.
[18] E. Vallat-Sauvain, U. Kroll, J. Meier, A. Shah, J. Pohl, J. Appl. Phys. 87 (2000) 3137.
[19] U. Kroll, J. Meier, P. Torres, J. Pohl, A. Shah, J. Non-Cryst. Solids 227–230 (1998) 68.
[20] J. Bailat, E. Vallat-Sauvain, L. Feitknecht, C. Droz, A. Shah, J. Non-Cryst. Solids 299–302 (2002) 1219.
[21] M. Kondo, T. Nishimto, M. Takai, S. Suzuki, Y. Nasuno, A. Matsuda, Technical Digest of the 12th International PVSEC, Jeju, Korea, 2001, p. 41.
[22] U. Graf, J. Meier, U. Kroll, J. Bailat, C. Droz, E. Vallat-Sauvain, A. Shah, Thin Solid Films, 2003, in press.
[23] J. Cifre, J. Bertomeu, J. Puigdollers, Appl. Phys. A 59 (1994) 645.
[24] S. Klein, F. Finger, R. Carius, O. Kluth, L.B. Neto, H. Wagner, M. Stutzmann, Proceedings of 17th EC PV Solar Energy Conference, Münich, 2001, p. 2965.
[25] N. Beck, P. Torres, J. Fric, Z. Remes, A. Poruba, H.A. Stuchlikova, A. Fejfar, N. Wyrsch, M. Vanecek, J. Kocka, A. Shah, Proc. Mater. Res. Soc. Symp. 452 (1997) 761.
[26] A. Poruba, A. Fejfar, Z. Remes, J. Springer, M. Vanecek, J. Kocka, J. Meier, P. Torres, A. Shah, J. Appl. Phys. 88 (2000) 148.
[27] M. Goerlitzer, N. Beck, P. Torres, U. Kroll, H. Keppner, J. Meier, J. Köhler, N. Wyrsch, A. Shah, Proc. Mater. Res. Soc. Symp. 467 (1997) 301.
[28] J.P. Kleider, C. Longeaud, R. Brüggemann, F. Houzé, Thin Solid Films 383 (2001) 57.
[29] H. Liu, M. Xu, Solid State Commun. 58 (1986) 601.
[30] S. Ray, S. Mukhopadhyay, T. Jana, R. Carius, J. Non-Cryst. Solids 299–302 (2002) 761.
[31] M. Goerlitzer, Ph.D Thesis, Université de Neuchâtel, 1998, ISBN 2-9700197–0–1.
[32] M. Goerlitzer, P. Torres, N. Beck, N. Wyrsch, H. Keppner, J. Pohl, A. Shah, J. Non-Cryst. Solids 227–230 (1998) 996.
[33] U. Kroll, J. Meier, A. Shah, S. Mikhailov, J. Weber, J. Appl. Phys. 80 (1996) 4971.
[34] N. Beck, N. Wyrsch, C. Hof, A. Shah, J. Appl. Phys. 79 (1996) 9361.
[35] C. Droz, M. Goerlitzer, N. Wyrsch, A. Shah, J. Non-Cryst. Solids 266–269 (2000) 319.
[36] A. Shah, E. Sauvain, J. Hubin, P. Pipoz, C. Hof, Philos. Mag. B 75 (1997) 925.
[37] M. Goerlitzer, N. Beck, P. Torres, J. Meier, N. Wyrsch, A. Shah, J. Appl. Phys. 80 (1996) 5111.
[38] N. Wyrsch, C. Droz, L. Feitknecht, J. Spitznagel, A. Shah, Proc. Mater. Res. Soc. Symp. 715 (2002) 363.
[39] N. Wyrsch, P. Torres, M. Goerlitzer, E. Vallat, U. Kroll, A. Shah, M. Vanecek, Solid State Phenomena 67–68 (1999) 89.
[40] V. Svrcek, I. Pelant, J. Kocka, P. Fojtik, B. Rezek, H. Stuchlikova, A. Fejfar, J. Stuchlik, A. Poruba, J. Tousek, J. Appl. Phys. 89 (2001) 1800.
[41] N. Wyrsch, C. Droz, L. Feitknecht, M. Goerlitzer, U. Kroll, J. Meier, P. Torres, E. Vallat-Sauvain, A. Shah, M. Vanecek, Proc. Mater. Res. Soc. Symp. 609 (2000) A15.1.
[42] Y. Chen, S. Wagner, Appl. Phys. Lett. 75 (1999) 1125.
[43] P. Torres, J. Meier, R. Flückiger, U. Kroll, J.A.A. Selvan, H. Keppner, A. Shah, S.D. Littlewood, I.E. Kelly, P. Giannoulès, Appl. Phys. Lett. 69 (1996) 1373.
[44] Y. Nasuno, M. Kondo, A. Matsuda, Appl. Phys. Lett. 78 (2001) 2330.
[45] J. Meier, S. Dubail, J. Cuperus, U. Kroll, R. Platz, P. Torres, J.A.A. Selvan, P. Pernet, N. Beck, N.P. Vaucher, C. Hof, D. Fischer, H. Keppner, A. Shah, J. Non-Cryst. Solids 227–230 (1998) 1250.

[46] J. Meier, E. Vallat-Sauvain, S. Dubail, U. Kroll, J. Dubail, S. Golay, L. Feitknecht, P. Torres, S. Fay, D. Fischer, A. Shah, Sol. Energy Mater. Sol. Cells 66 (2001) 73.
[47] K. Yamamoto, M. Yoshimi, T. Suzuki, Y. Tawada, Y. Okamoto, A. Nakajima, Proceedings of the Second World Conference on Photovoltaic Energy Conversion, Vienna, 1998, p. 1284.
[48] J. Meier, H. Keppner, S. Dubail, U. Kroll, P. Torres, P. Pernet, Y. Ziegler, J.A.A. Selvan, J. Cuperus, D. Fischer, A. Shah, Proc. Mater. Res. Soc. Symp. 507 (1998) 139.
[49] K. Saito, M. Sano, A. Sakai, R. Hayashi, K. Ogawa, Technical Digest of the 12th International PVSEC, Jeju, Korea, 2001, p. 429.
[50] J. Meier, R. Flückiger, H. Keppner, M. Göetz, A. Shah, Proceedings of the 12th EC PV Solar Energy Conference, Amsterdam, 1994, p. 1237.
[51] H. Keppner, J. Meier, P. Torres, D. Fischer, A. Shah, Appl. Phys. A 69 (1999) 169.
[52] T.J. Coutts, J.S. Ward, D.L. Young, T.A. Gessert, R. Noufi, Technical Digest of the 12th International PVSEC, Jeju, Korea, 2001, p. 277.
[53] W. Ma, T. Horiuchi, C.C. Lim, K. Goda, I.I. Okamoto, Y. Hamakawa, Proceedings of the 23rd IEEE Photovoltaic Specialists Conference, 1993, p. 833.
[54] J. Meier, S. Dubail, R. Flückiger, D. Fischer, H. Keppner, A. Shah, Proceedings of the First World Conference on Photovoltaic Energy Conversion, Hawaii, USA, 1994, p. 409.
[55] J. Meier, P. Torres, R. Platz, S. Dubail, U. Kroll, J.A.A. Selvan, N. Pellaton-Vaucher, C. Hof, D. Fischer, H. Keppner, A. Shah, K.D. Ufert, Sol. Energy Mater. Sol. Cells 49 (1997) 35.
[56] K. Yamamoto, M. Yoshimi, T. Sawada, A. Nakajima, K. Hayashi, T. Suezaki, H. Takata, Y. Tawada, Technical Digest of the 12th International PVSEC, Jeju, Korea, 2001, p. 547.
[57] Y. Tawada, H. Yamagishi, K. Yamamoto, Sol Energy Mater. Sol. Cells, this issue.
[58] J. Meier, J. Spitznagel, S. Faÿ, C. Bucher, U. Graf, U. Kroll, S. Dubail, A. Shah, Proceedings of the 29th IEEE Photovoltaic Specialists Conference, New Orleans, 2002, p. 1118.
[59] D. Fischer, S. Dubail, J.A.A. Selvan, N.P. Vaucher, R. Platz, C. Hof, U. Kroll, J. Meier, P. Torres, H. Keppner, N. Wyrsch, M. Goetz, A. Shah, K.D. Ufert, Proceedings of the 25th IEEE Photovoltaic Specialists Conference, Washington D.C, 1996, p. 1053.
[60] N. Pellaton-Vaucher, J.L. Nagel, R. Platz, D. Fischer, A. Shah, Proceedings of the Second World Conference on Photovoltaic Energy Conversion, Vienna, 1998, p. 728.